

# A Versatile Non-Fouling Multi-step Flow Reactor Platform: Demonstration for Partial Oxidation Synthesis of Iron Oxide Nanoparticles

Maximilian O. Besenhard,<sup>\*a</sup> Sayan Pal,<sup>a</sup> Liudmyla Storozhuk,<sup>b</sup> Simon Dawes,<sup>a</sup> Nguyen T.K. Thanh,<sup>b,c</sup> Laura Norfolk,<sup>d</sup>

Sarah Staniland,<sup>d</sup> Asterios Gavriilidis<sup>\*a</sup>

<sup>a</sup> Department of Chemical Engineering, University College London, Torrington Place, London, WC1E 7JE, UK

<sup>b</sup> Biophysics Group, Department of Physics and Astronomy, University College London, Gower Street, London, WC1E 6BT, UK

<sup>c</sup> UCL Healthcare Biomagnetics and Nanomaterials Laboratories, University College London, 21 Albemarle Street, London, W1S 4BS, UK

<sup>d</sup> Department of Chemistry, The University of Sheffield, Dainton Building, Brook Hill, Sheffield, S3 7HF, UK

\* Corresponding authors: *m.besenhard@ucl.ac.uk* and *a.gavriilidis@ucl.ac.uk*

## Supporting Information

### Contents:

<b>SI1 Chemicals, materials and manufacturing</b>	<b>2</b>
<b>SI2 Additional details of three-phase reactor platform</b>	<b>4</b>
SI2.1 Platform components	4
SI2.2 Platform operating flow rates range	8
SI2.3 Platform operation recommendations	12
<b>SI3 Batch synthesis studies</b>	<b>13</b>
SI3.1 Estimation of magnetite/maghemite formation timescales	13
SI3.2 Citric acid solution addition for improved colloidal stability	15
<b>SI4 Single phase flow synthesis</b>	<b>17</b>
<b>SI5 Flow synthesis reproducibility</b>	<b>18</b>

## S11 Chemicals, materials and manufacturing

The materials used for the flow reactor are listed in **Table S1**. All chemicals used for this work are listed in

**Table S2**. The manufacturing of the droplet generator and T-units is described at the end of this section.

**Table S1:** Details of reactor components used

Compound	Details/comments	Material/Model	Product Number (manufacturer)
Syringe pump(s)	Each pump can fit 2 syringes		Legato210, KD Scientific
Syringes	50 ml	Glass	009760 (SGE syringes, TRAJAN)
Syringes	10 ml	Glass	008960 (SGE syringes, TRAJAN)
Mass flow controller	0.1-5 ml <sub>n</sub> /min	EL-FLOW Prestige	FG-200CV-RAD-22-V-DA-A1V (Bronkhorst)
Tubing (used to connect pumps with reactor elements)	1.0 mm ID, 1.6 mm OD	Polytetrafluoroethylene (PTFE)	JR-T-6807-M25 (VICI Jour)
Tubing (used for reactor)	1.0 mm ID, 1.6 mm OD	Perfluoroalkoxy alkane (PFA)	JR-T-4007-M25 (VICI Jour)
Standard connector used to mix TEPA and precursor solution	0.5 mm channel diameter	Polyetheretherketone (PEEK)	P-712 (IDEX Health Science)
Standard connectors used to connect platform elements	Flangeless fitting nut for 1/6" tubing with 1/4-28 flat-bottom thread	Polyetheretherketone (PEEK)	P-230 (IDEX Health Science)
	Flangeless ferrule for 1/6" tubing with 1/4-28 flat-bottom thread	Ethylentetrafluoroethylene (ETFE)	P-200 (IDEX Health Science)
Pressure pump	Used to purge solutions with N <sub>2</sub> and maintain inert atmosphere during batch studies.	4 channel system equipped with MFS4 flow meter	OB1 (Elveflow)
Magnetic stirrer and heater	ETS-D5 temperature controller		C-MAG HS 7 (IKA)
Water bath	Crystallisation dish 90 mm height, 190 mm diameter	Glass (Duran®)	216-1868 (VWR)
Droplet generator	All inlets and outlets had a channel diameter of 1 mm except gas inlet.	Polycarbonate (PC) sheets (9.5 mm thick) and PFA tubing inserted	Material provided by Direct Plastics and Polyflon

T-unit for reagent addition into droplets	The inner channel diameter was drilled to 1 mm. The addition channel was smaller.	Moulded fluorinated ethylene propylene (FEP) sheets (9.5 mm thick)	Material provided by Polyflon
---	---	--	-------------------------------

**Table S2:** Details of chemicals used

Compound	Purchased from	Brand	Product Nr. (Quantity)
Iron(II) sulfate heptahydrate ( $\text{FeSO}_4 \cdot 7\text{H}_2\text{O}$ )	Merck UK	Honeywell/Fluka	215422 (250 g)
Potassium nitrate ( $\text{KNO}_3$ )	Merck UK	Honeywell	P8394 (500 g)
Potassium hydroxide (KOH) 0.1 M solution	Merck UK	Sigma-Aldrich	61699 (1 l)
Citric acid monohydrate ( $\text{C}_6\text{H}_8\text{O}_7 \cdot \text{H}_2\text{O}$ )	Merck UK	Sigma-Aldrich	C1909 (500 g)
Tetraethylenepentamine (TEPA)	Merck UK	Sigma-Aldrich	T11509 (100 g)
Sulphuric acid ( $\text{H}_2\text{SO}_4$ )	Merck UK	Honeywell/Fluka	319589 (2 l)
Heptane ( $\text{C}_7\text{H}_{16}$ )	LP Chemicals	LP Chemicals	UN1206 (2.5 l)
IPA (used for cleaning)	Merck UK	Sigma Aldrich	59300

The droplet generators and T-units were manufactured in UCL's High Precision Design & Fabrication Facility using flat stock 0.9-1.5 mm thick plastic sheets as starting material. The bodies of the reactor elements were machined from these plastic sheets using a Haas TL1 Vertical machining centre and programmed using Edgcam (CAM). A pocket (window for visual inspection) was machined into all elements (except the polycarbonate ones (as they were sufficiently transparent) by thinning the sheets down to the thickness of the tubing that was being used for the flow syntheses, i.e., the distance between the main channel and the outside in these pockets was made  $\sim 0.25$  mm. The 1 mm holes (main channels) in the elements were drilled at 0.90 mm and reamed at 1 mm diameter for accuracy and hole finish. The thinner holes in the T-units were drilled likewise, using thinner drill bits. The flexible gas injection nozzle system for the droplet generator was machined using Haas VMC and hand finished using a manual lathe. The stainless-steel tube was adapted from a 316 stainless steel syringe needle and inserted into the nozzle using an interference fit to secure in place.

## S12 Additional details of three-phase reactor platform

### S12.1 Platform components

This section provides additional high-speed camera images showing (with more steps/images) the three-phase droplet generation steps using the transparent polycarbonate element (see **Figure S1**, 1<sup>st</sup> aqueous stream with blue dye), as well as the reagent addition into aqueous droplets (2<sup>nd</sup> aqueous stream with red dye) at different flow rates (see **Figure S2** & **Figure S3**). Also shown are images where the reagent/solution addition into droplets failed because the T-unit was made of a less hydrophobic plastic, i.e., polycarbonate (see **Figure S4**). **Figure S5** shows pictures of the reactor elements. These images/videos were recorded placing the reactor elements on a white LED square panel providing the backlight.

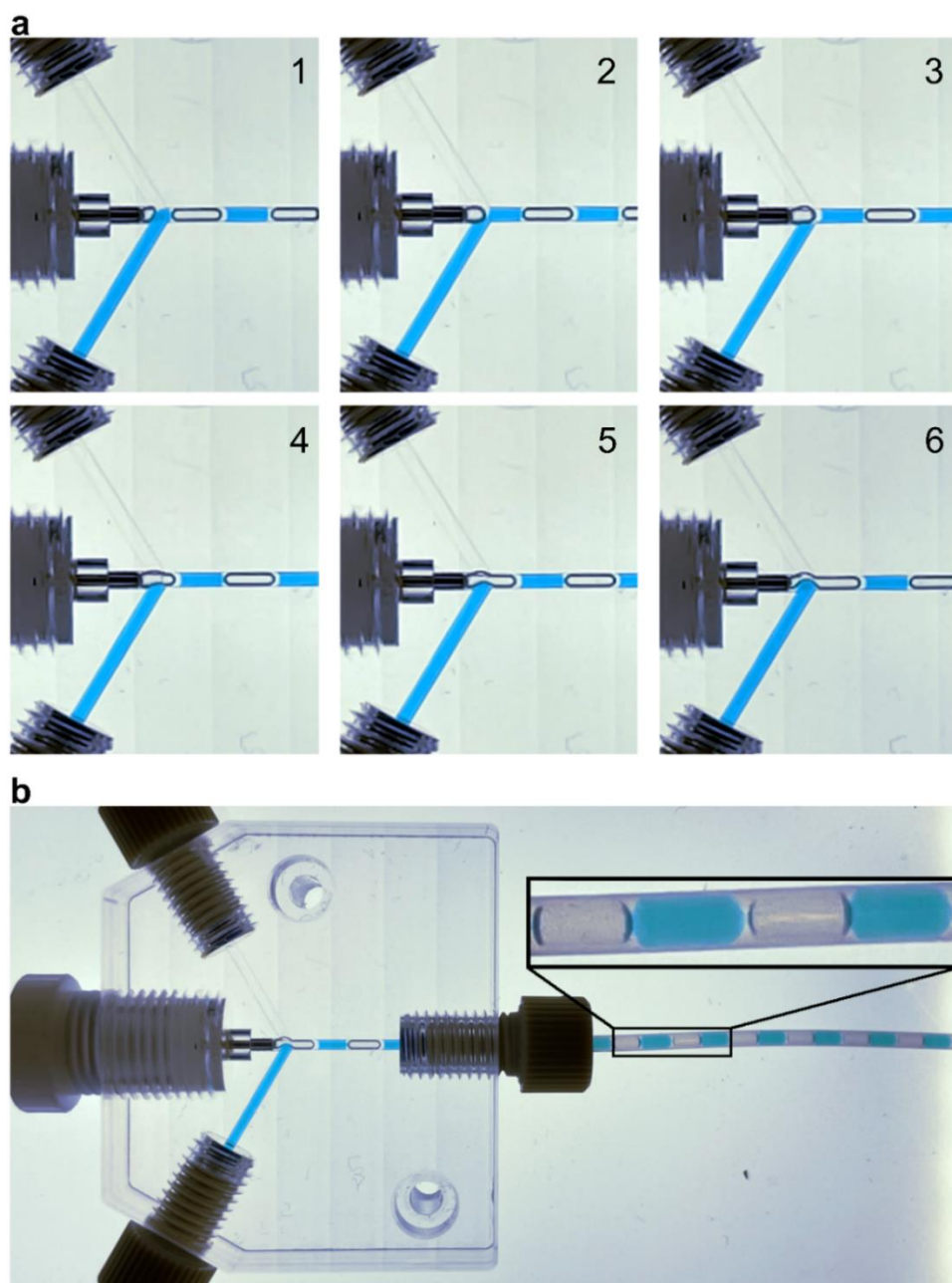


**Figure S1:** (a) Consecutive images showing droplet formation (flow direction: left to right). The images were taken from the high-speed camera video provided in the ESI (Droplet\_generation); 1<sup>st</sup> aqueous phase with blue dye. (b) Droplet generator was made of polycarbonate. The insert (magnified region of the tube) shows that the three-phase flow has become well-ordered gas-liquid-liquid segmented flow. Blue dye 0.4 ml/min, N<sub>2</sub> 0.4 ml<sub>v</sub>/min, heptane 0.1 ml/min.

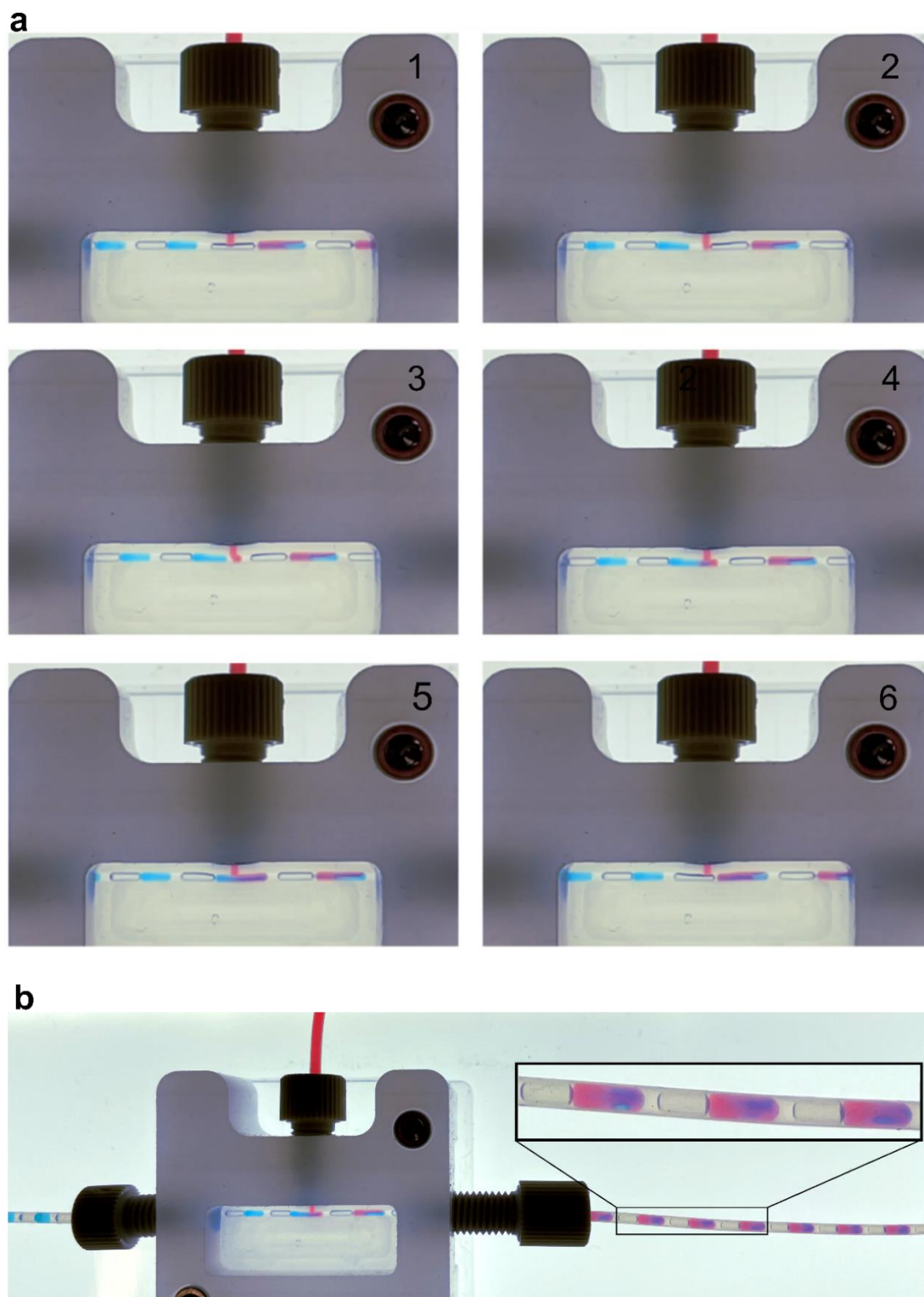


**Figure S2:** (a) Consecutive images showing reagent addition into droplets (flow direction: left to right, 1<sup>st</sup> aqueous stream: blue dye 0.4 ml/min, 2<sup>nd</sup> aqueous stream: red dye 0.2 ml/min). The images were taken from the high-speed camera video provided in the ESI (Droplet\_addition\_1, shown in slow motion); 2<sup>nd</sup> aqueous stream with red dye. (b) T-unit made of PFA. The insert (magnified region of the tube) shows how mixing continues once reagents were added. The heptane flow rate was 0.2 ml/min which is twice as much as used for the images shown in Figure S1, hence the heptane phase becomes more apparent, i.e., the gap between the droplet and the gas bubble is bigger.

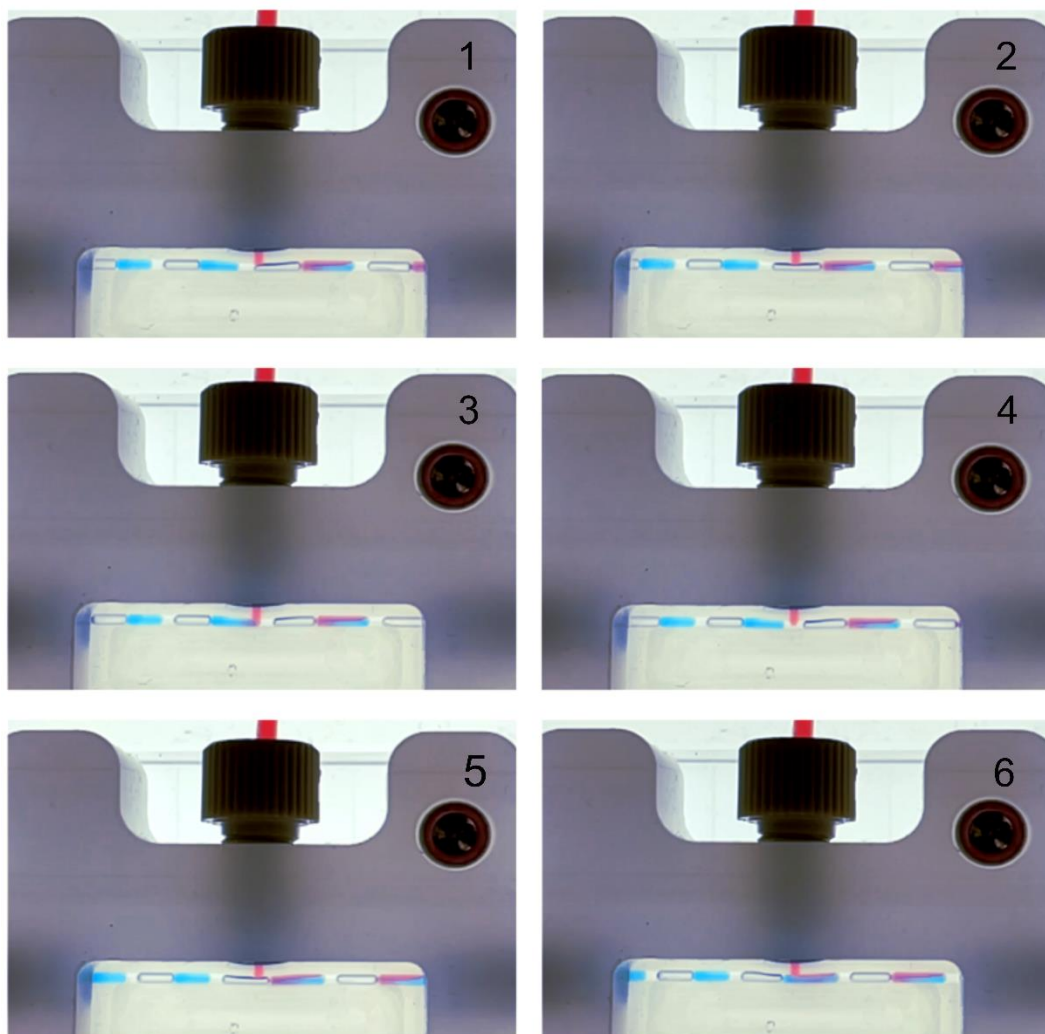


**Figure S3:** Consecutive images showing reagent addition into droplets (flow direction: left to right), 1<sup>st</sup> aqueous stream: blue dye 0.4 ml/min, 2<sup>nd</sup> aqueous stream: red dye 0.1 ml/min). The images were taken from the high-speed camera video provided in the ESI (Droplet\_addition\_2, shown in slow motion). The heptane flow rate was 0.2 ml/min.

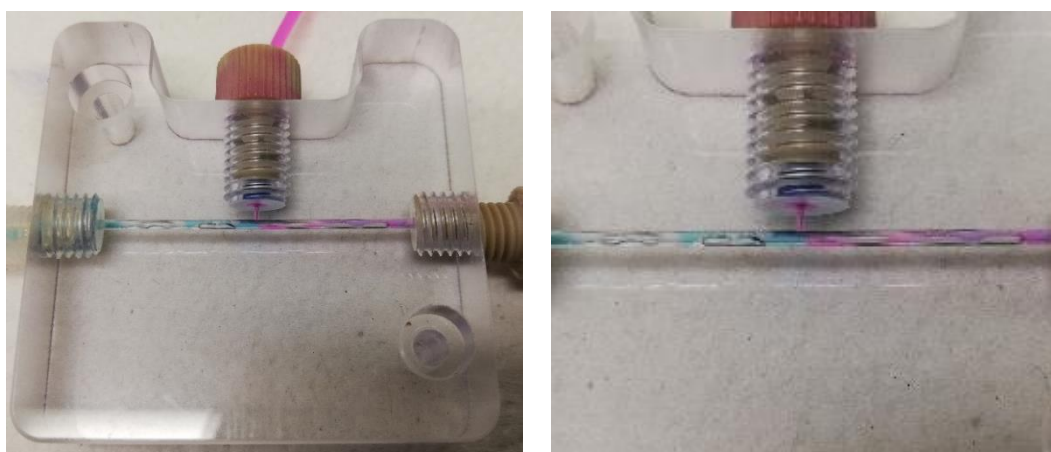


**Figure S4:** Image showing unsuccessful reagent addition into droplets (flow direction: left to right, 1<sup>st</sup> aqueous stream: blue dye 0.4 ml/min, 2<sup>nd</sup> aqueous stream: red dye 0.3 ml/min) using a polycarbonate T-unit. Aqueous stream came in touch with the wall and small residues remained, which cannot be removed by the oil/continuous phase. These residues caused instabilities of the three-phase segmentation in the channel, which made the controlled reagent addition into droplets impossible.

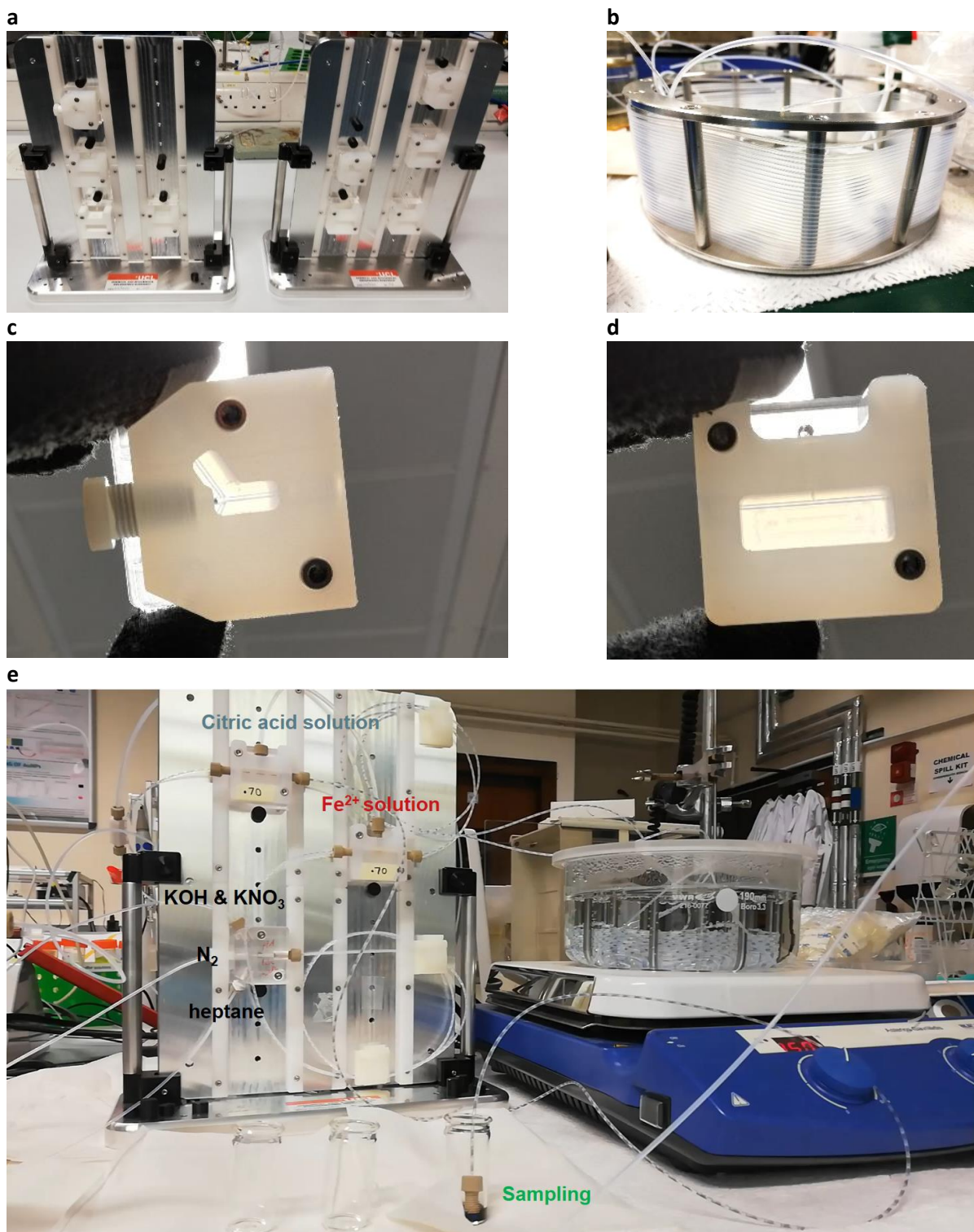


**Figure S5:** Pictures of the reactor platform elements. **(a)** Stands for reactor elements (with droplet generation T-units made of FEP mounted). Each stand allows to slot in multiple elements in two columns at adjustable heights. **(b)** Residence time module, consisting of metal tube holder with PFA tubing (here max. length of ca. 15 m) for immersion in the heated water bath. **(c)** Droplet generator made of FEP with adjustable metal nozzle (positioned at its minimum insertion) held against a light-source. **(d)** T-unit for reagent addition into droplets made of FEP held against a light-source. **(e)** Three-phase reactor platform during partial oxidation synthesis.

## S12.2 Platform operating flow rates range

To demonstrate the flexibility of the three-phase reactor platform, the set-up used for the IONP synthesis (see **Figure 2**) was operated at different flow rates and using coloured aqueous solutions to visualise the reagent addition into droplets. The 1<sup>st</sup> aqueous stream was coloured with blue dye and the 2<sup>nd</sup> aqueous stream with red dye. The images/videos were recorded placing the T-unit for the 1<sup>st</sup> droplet reagent addition on an LED square panel backlight with an antiglare diffuser.

**Figure S6** shows the 1<sup>st</sup> reagent addition into droplets at the flow rates for heptane, nitrogen and the 1<sup>st</sup> aqueous phase (blue dye: 0.4 ml/min) used for the IONP synthesis, but varying the feed rate for the 2<sup>nd</sup> aqueous stream (red dye: 0.05-0.4 ml/min). The addition into droplets was robust at 2<sup>nd</sup> aqueous stream flow rates < 0.4 ml/min. At the highest flow rate tested, i.e., 0.4 ml/min (1<sup>st</sup>:2<sup>nd</sup> aqueous phase flow rate ratio = 1:1), a small fraction of the 2<sup>nd</sup> aqueous stream feed did not merge with the existing/primary aqueous droplets and formed new droplets dividing the gas bubble (see insert in bottom image in **Figure S6**). These newly formed droplets, however, merged with the primary aqueous slugs/droplets quickly and homogeneous three-phase segmented flow exited the T-unit for the 1<sup>st</sup> droplet reagent addition. The corresponding video is provided in the ESI (see *Droplet\_addition\_varying\_feedrates*).

The set-up was then operated at half (blue dye: 0.2 ml/min, red dye: 0.025-0.2 ml/min) and double (blue dye: 0.8 ml/min, red dye: 0.1-0.8 ml/min) the flow rates used for the IONP synthesis while varying the feed rates for the 2<sup>nd</sup> aqueous stream. The operation at halved (see **Figure S7** and the video *Droplet\_addition\_varying\_feedrates\_lower*) and doubled (see **Figure S8** and the video *Droplet\_addition\_varying\_feedrates\_higher*) flow rates showed the same behaviour. The addition into slugs/droplets was robust as long as the flow rate of the 2<sup>nd</sup> aqueous stream was lower than the flow rate of the 1<sup>st</sup> aqueous stream. When the 1<sup>st</sup>:2<sup>nd</sup> aqueous phase flow rate ratio was 1:1, new droplets formed which divided the gas bubble (see inserts in bottom images in **Figure S7** and **Figure S8**). Similarly to the base case, also for the halved and doubled flow rates the newly formed droplets merged with the primary aqueous droplets and homogeneous three-phase segmented flow exited the T-unit for the 1<sup>st</sup> droplet reagent addition.

These studies revealed the flexibility of the three-phase reactor platform in terms of the flow rates. Robust feeding of new reagent solutions into droplets (using the same multi-stage set-up used for the IONP synthesis described) was possible as long as the 1<sup>st</sup>:2<sup>nd</sup> aqueous phase feed rate ratio was < 1:1. This is remarkable, considering that the volume of the dispersed phase, i.e., the droplets/slugs of the reactive liquid, could almost be doubled in a single reagent addition step. The batch equivalent of this upper boundary for the aqueous phase feed rate ratio would be a rapid doubling of the volume, e.g. in a flask, due to a single reagent solution addition step. The platform did also prove its flexibility with respect to the total flow rate, showing robust reagent addition into droplet/slugs for all tested total flow rates, i.e., between 0.2+0.025 ml/min (1<sup>st</sup>+2<sup>nd</sup> aqueous phase) and 0.8+0.6 ml/min (1<sup>st</sup>+2<sup>nd</sup> aqueous phase).

Continuous phase (heptane): 0.15 ml/min; Gas (nitrogen): 0.4 ml<sub>n</sub>/min

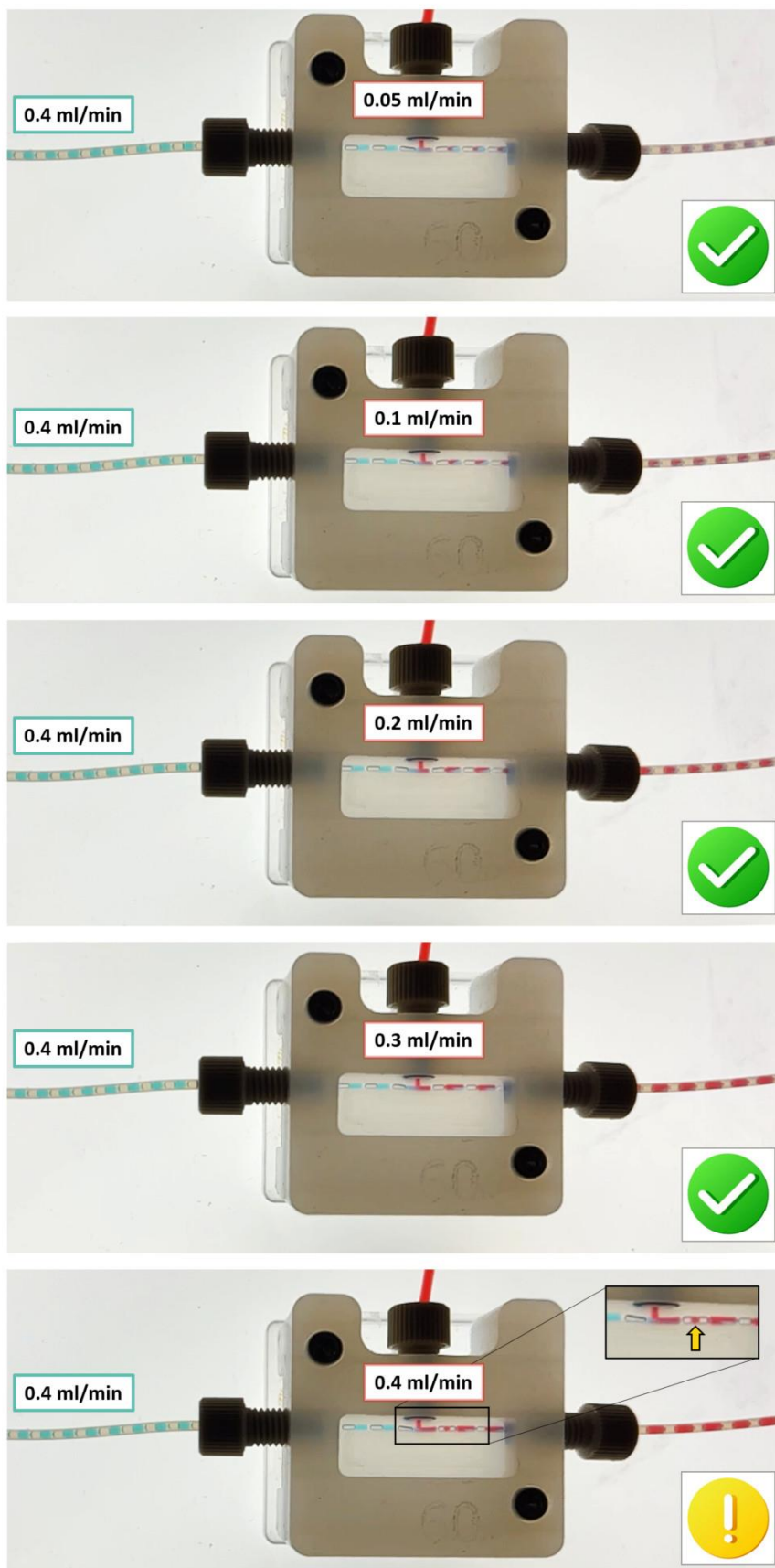


**Figure S6:** Images during reagent addition into droplets at the flow rates used for IONP synthesis (1<sup>st</sup> aqueous stream/blue dye: 0.4 ml/min) and varying 2<sup>nd</sup> aqueous stream/red dye feed rates: 0.05-0.4 ml/min.

Continuous phase (heptane): **0.075 ml/min**; Gas (nitrogen): **0.2 ml<sub>n</sub>/min**

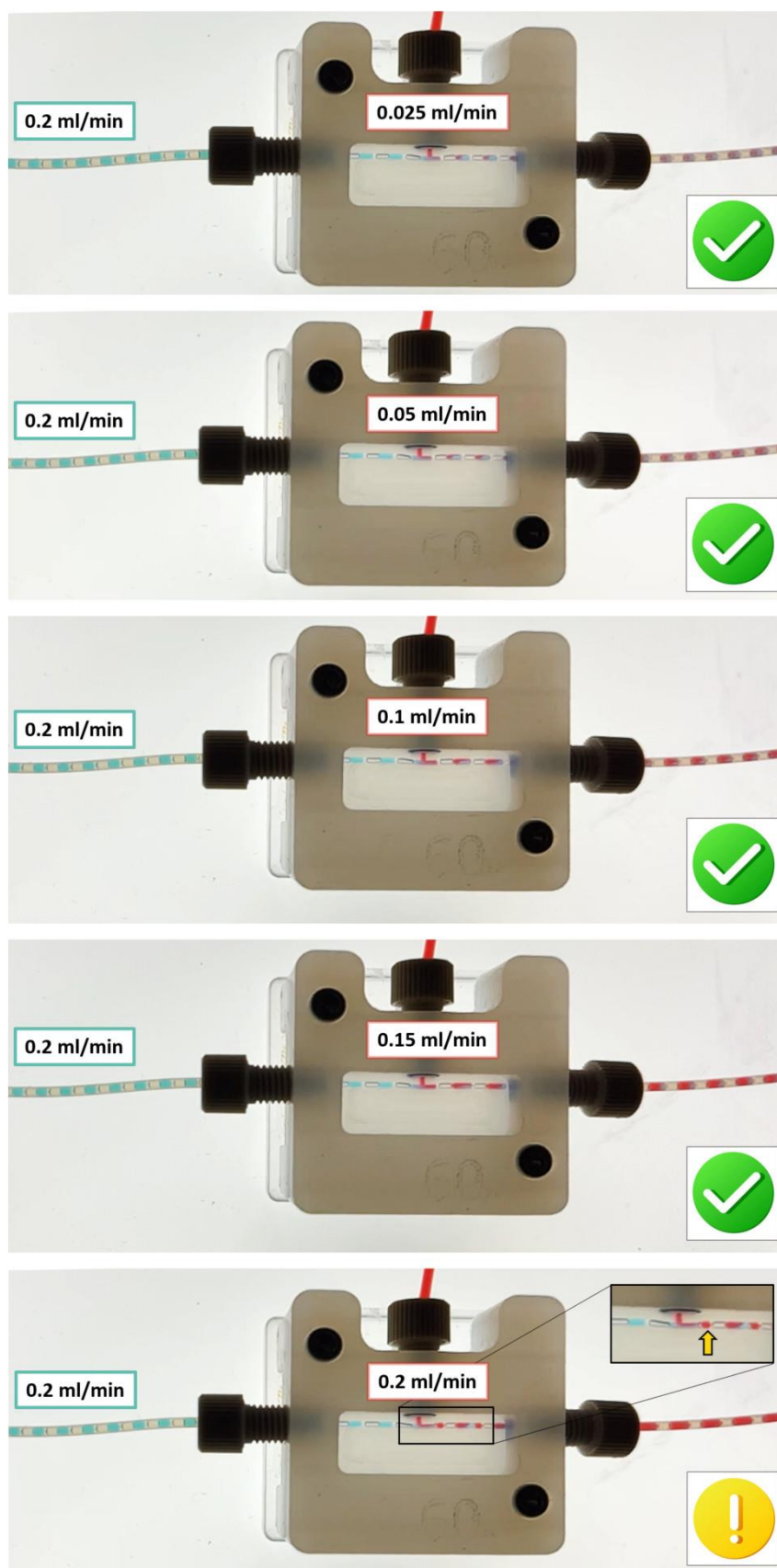


**Figure S7:** Images during reagent addition into droplets at half the flow rates used for IONP synthesis (1<sup>st</sup> aqueous stream/blue dye: **0.2 ml/min**) and varying 2<sup>nd</sup> aqueous stream/red dye feed rates: **0.025-0.2 ml/min**.

Continuous phase (heptane): 0.3 ml/min; Gas (nitrogen): 0.8 ml<sub>n</sub>/min

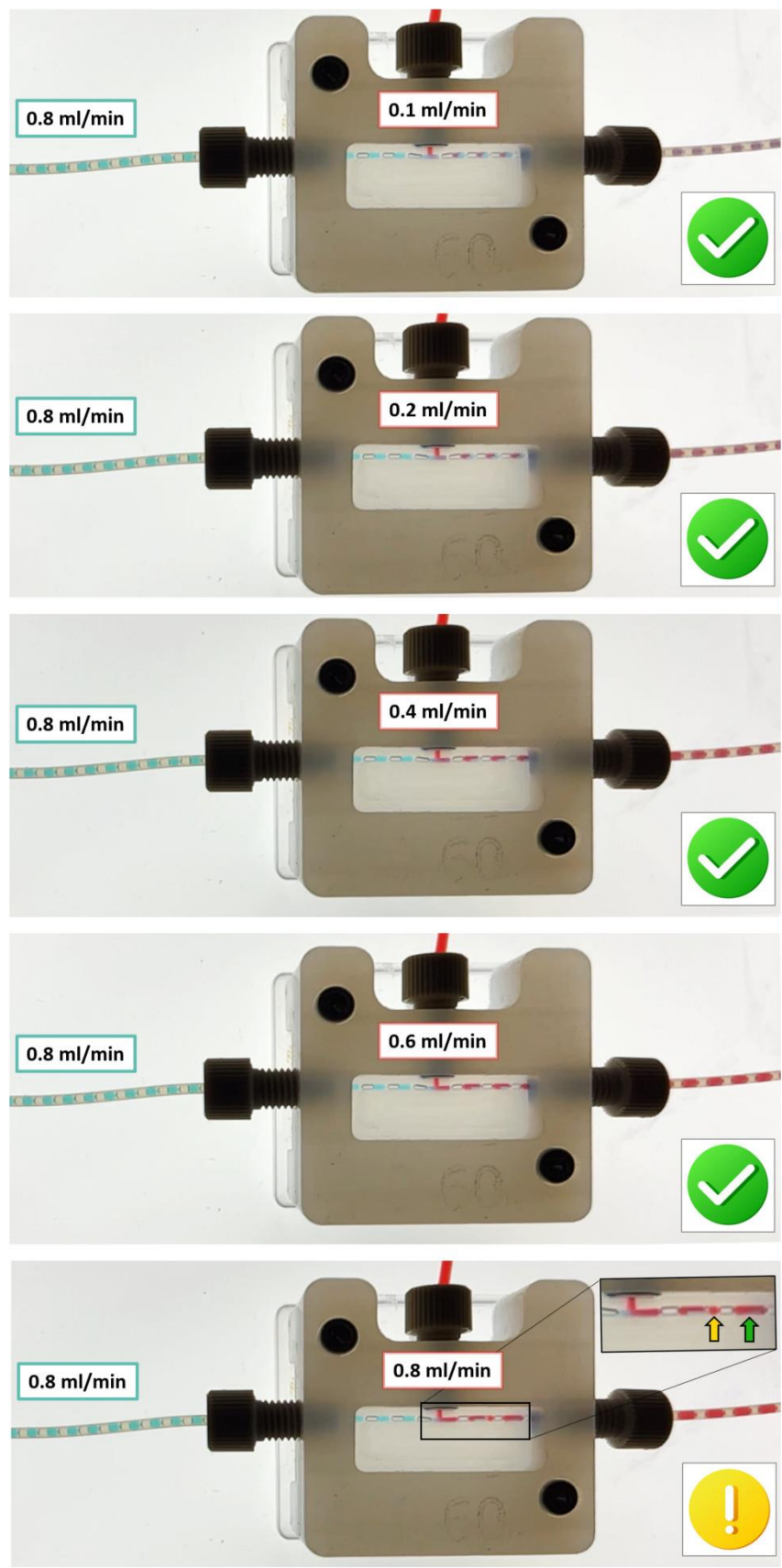


**Figure S8:** Images during reagent addition into droplets at double the flow rates used for IONP synthesis (1<sup>st</sup> aqueous stream/blue dye: **0.8 ml/min**) and varying 2<sup>nd</sup> aqueous stream/red dye feed rates: **0.1-0.8 ml/min**.

### **S12.3 Platform operation recommendations**

The points below should be considered as recommendations to establish steady state operations easily using the three-phase reactor platform. Once steady state operation is established, the process is robust. In general, the operation is simple. When having heated segments, however, the expansion of gas due to the temperature increase can cause pressure fluctuations (i.e., inlet-outlet pressure differences) which make it more difficult to reach steady state operation quickly. Therefore, we recommend the following:

- Always start the reactor operation by feeding the gas phase, preferably via an accurate mass flow controller, before starting the pumps feeding the oil/continuous phase and the aqueous liquids. Also, stopping the gas feed should be the last thing after operating the reactor, i.e., the liquid feeding pumps should be turned off before the mass flow controller. However, make sure you don't allow gas to enter into any of the liquid reservoirs (which is easy to avoid when using syringe pumps).
- Start feeding the organic/continuous phase before feeding the aqueous liquids. However, make sure the organic/continuous phase does not enter the channels connecting the aqueous phase reservoirs with the reactor elements. When using syringe pumps this can be done, e.g., by feeding all aqueous liquids and stopping the feeds before the aqueous solutions enter the platform elements, i.e., droplet generator or T-units.
- When using heated segments, it is recommended to increase temperatures (e.g., from room temperature) after stable three-phase segmentation is established throughout the reactor at a lower temperature.
- When changing flow rates, make sure the new flow rates do not vary significantly from previous flow rates. If they do, it might be best to increase or decrease the flow rates in multiple steps (separated by  $\sim 1$  residence time). For operations at higher flow rates (especially of the reagent solution(s) to be added after segmentation), the gas bubble size should be reduced.
- Operating against a back pressure can help to stabilise the three-phase segmented flow when using heated segments and slowly increasing the temperature is not an option. For example, samples could be collected directly into pressurised vessels (note that most glass vessels used for BPR are rated to 1.5 bar max.).
- Having a higher pressure drop at the end of the reactor (e.g., through additional T-units or tubing with a reduced inner diameter closer to the reactor outlet) will help to establish steady state operation quickly. This will reduce the effect of pressure drop fluctuations caused by irregular three phase flow segmentation when establishing the steady state operation or switching between steady states.
- For operations requiring long tubing and/or high flow rates (e.g., flow rates  $> 2$  ml/min using tube lengths  $> 5$  m; ID 1 mm), high gas/liquid flow rate ratios should be used. This is to reduce the pressure drop in the reactor. Note that three-phase segmented flow has a significantly larger pressure drop per tube length than single phase and liquid-liquid or gas-liquid segmented flows for the same total flow rate.
- Use a cleaning solution in which the aqueous and the organic/continuous phase are at least partially soluble (e.g., isopropyl alcohol or ethanol when dispersing aqueous solutions in a continuous heptane phase). When cleaning the reactor, reduce the gas flow rate (but not to 0 ml/min).

## S13 Batch synthesis studies

### S13.1 Estimation of magnetite/maghemite formation timescales

Translating the partial oxidation method into flow required knowledge of the particle formation kinetics. More specifically, an estimation of the timescale to form magnetite/maghemite at the different temperatures was needed to set the residence time in the flow reactor. Therefore, partial oxidation syntheses were performed in batch at different temperatures while monitoring the solution appearance, as well as using a hand-held magnet to probe for the presence of magnetite/maghemite. This is no precise method and only served to estimate the time needed to form magnetite/maghemite.

The three solutions used for these studies were (1) a 0.45 M FeSO<sub>4</sub> precursor solution, (2) a 1 M KOH solution, and (3) a 0.5 M KNO<sub>3</sub> solution. All solutions were prepared freshly before each experiment using N<sub>2</sub> purged water and purged again after solution preparation for > 1 h before the experiment. Details of all chemicals used including product numbers are listed in

Table S2.

The batch experiments were performed as follows. First, 2.5 ml of solution 1 and 2.5 ml of solution 2 were mixed in a flask (kept under N<sub>2</sub> atmosphere) at room temperature (ca. 22 °C) to initiate the hydroxide precipitation. 1 min later, 20 ml of solution 3 were added. After stirring for 4 min at room temperature, the flask was immersed (under stirring and N<sub>2</sub> atmosphere) in a heated water bath to reach and maintain the reaction temperature set. Without the heating step, no material could be separated via a handheld magnet (see **Figure S9a**), even after hours (results not shown). It should be noted that the batch synthesis was performed without stabiliser and does not yield colloiddally stable particles. Hence, magnetic particles formed are likely to agglomerate making their separation via a handheld magnet easy. Only after heating, the solution turned black over time and magnetic material formed (see **Figure S9b**).

The results can be summarised as follows with times referring to the immersion in the heated water bath (= 0 min):

#### Batch partial oxidation at 80 °C

Solution turns dark green after 1-2 min, and black after ~3 min. Particle separation via a magnet was possible, indicating that magnetite/maghemite has formed.

#### Batch partial oxidation at 60 °C

Solution turns dark green after 3-5 min, and black after ~8 min. Particle separation via a magnet was possible then, indicating that magnetite/maghemite has formed.

#### Batch partial oxidation at 40 °C

Solution turns dark green after 9-11 min, and black after ~20 min. Particle separation via a magnet was possible, indicating that magnetite/maghemite has formed.

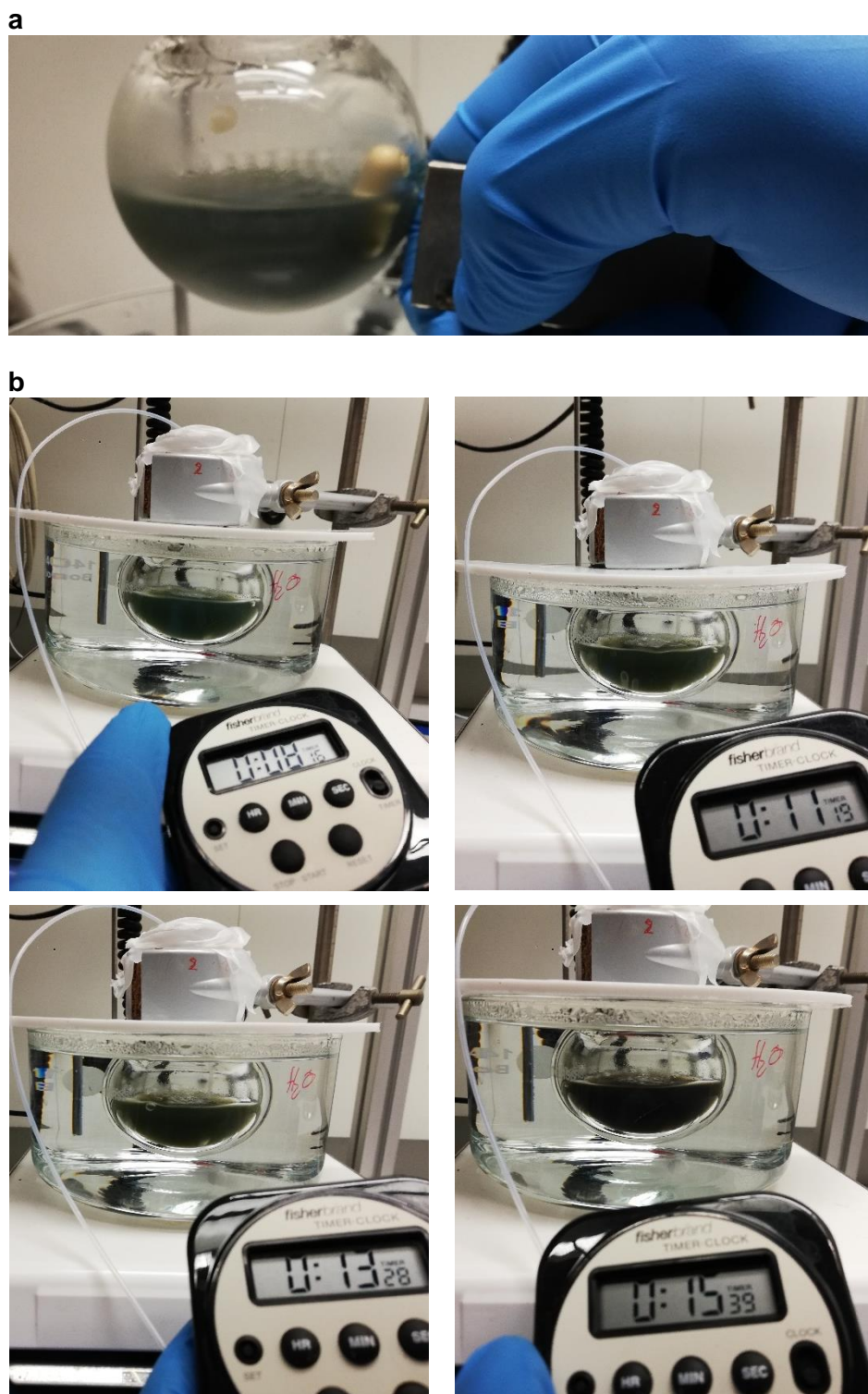


**Figure S9:** (a) Flask with precipitated solution (4 min after adding the  $\text{KNO}_3$  solution (3), no heating) next to handheld magnet. No attraction of particles is apparent. (b) Change in appearance with time at 60 °C. Note, the timer shown in the images was started after mixing solution (1) and (2), i.e., 5 min before initiating heating.

### S13.2 Citric acid solution addition for improved colloidal stability

Previous studies on co-precipitation syntheses revealed the importance of the quantity and timing (especially when the magnetite/maghemite formation is not complete) of citric acid addition for the size and colloidal stability of IONPs. Following initial studies on the amount of 0.64 M citric acid solution added to the 25 ml of IONP solutions (synthesised as described in the previous section) before dissolving the particles, the following batch studies were performed. Different amounts (i.e., 0.5 and 0.75 ml of 0.64 M citric acid solution) were added during the synthesis performed at 60 °C at different times (i.e., 10 and 15 min after initiating heating). The colloidal stability of IONP solutions synthesised with citric acid solution added 10 min after initiating heating showed good colloidal stability. However, TEM analysis (see **Figure S10a** and **b**) indicated that the transition to magnetite/maghemite was not complete as shown by the low contrast and needle shaped particles observed. This is in agreement with XRD analysis showing peaks that cannot be assigned to the inverse spinel structure of magnetite/maghemite (see **Figure S11**). TEM and XRD analysis of IONP solutions synthesised with citric acid solution being added 15 min after initiating heating (see **Figure S10c** and **d** and **Figure S11**) showed no signs of incomplete magnetite/maghemite formation, but a significantly reduced colloidal stability. It should be noted that colloidal stability was tested after 8 min of ultra-sonication.

These batch studies indicate that i) citric acid addition alone (no other stabiliser added) is not sufficient to achieve colloidal stability and that ii) the time of citric acid addition is important (too early yields incomplete magnetite/maghemite formation and too late allows magnetite/maghemite particles to aggregate).

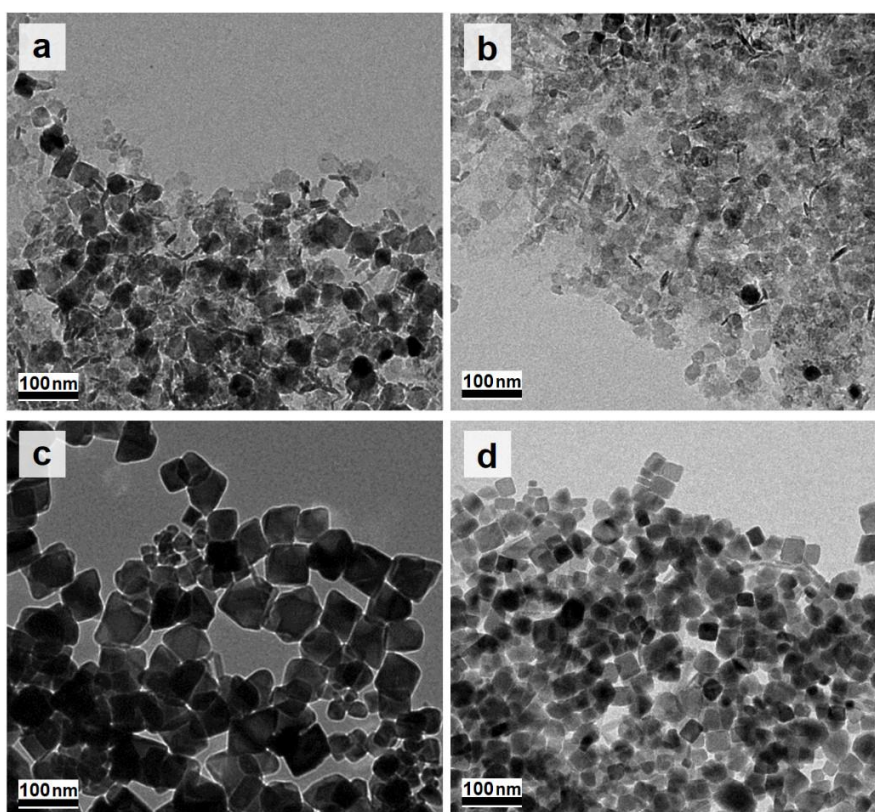


**Figure S10:** TEM images of IONPs synthesised in batch with different volumes of 0.64 M citric acid solution added at different times (always added to 25 ml; 2.5 ml of solution 1 and 2 and 20 ml of solution 3, see previous section) at 60 °C. (a) 0.5 ml added 10 min after initiation of heating, (b) 0.75 ml added 10 min after initiation of heating, (c) 0.5 ml added 15 min after initiation of heating, (d) 0.75 ml added 15 min after initiation of heating.

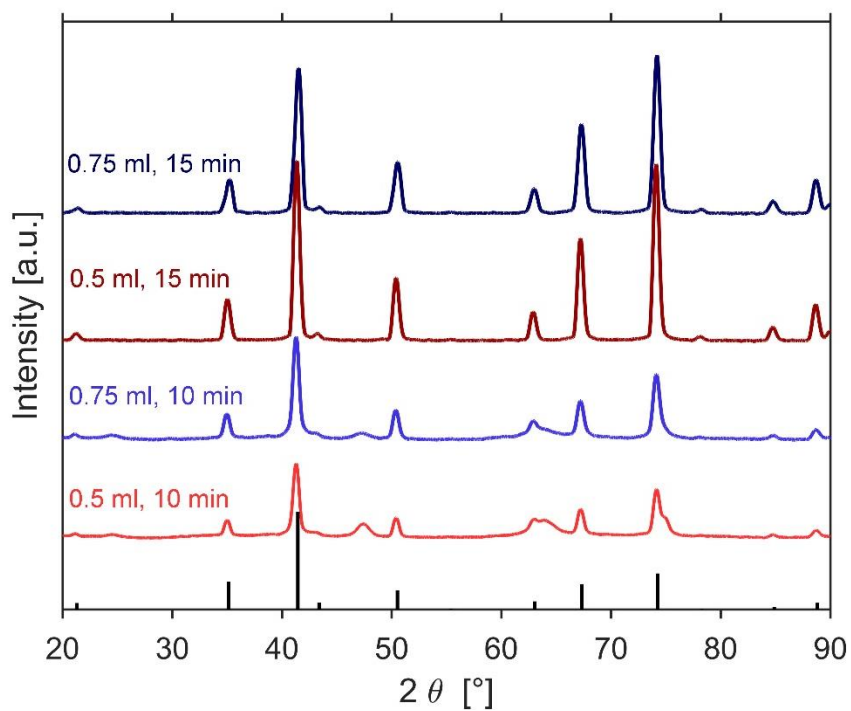


**Figure S11:** XRD patterns of IONPs synthesised in batch with different volumes of 0.64 M citric acid solution added at different times (always added to 25 ml; 2.5 ml of solution 1 and 2 and 20 ml of solution 3, see previous section) at 60 °C. The black bars at the bottom correspond to the reference pattern of the inverse spinel structure (magnetite: PDF ref. 03-065-3107).

#### S14 Single phase flow synthesis

A single-phase flow system was tested for comparison. The aim was to investigate if the synthesis can be performed in simple capillary based reactor systems without fouling or clogging the reactor. Different mixers such as standard T-Mixers (P-716, IDEX Health Science) as well as micro mixers (P-890 and P-727, IDEX Health Science) were used to mix at equal flow rates (1) a 0.45 M  $\text{FeSO}_4$  precursor solution with (2) a 1 M KOH solution, i.e., the same concentrations as used for the batch synthesis studies without citric acid addition. The mixers were followed by PTFE or PFA tubing (ID = 1 mm), which was either straight or coiled as coaxial flow inverter.

For all single-phase reactor systems tested (see **Figure S12** for an example), reactor fouling in the tubing was obvious within < 1 min (even without adding (3) the 0.5 M  $\text{KNO}_3$  solution), and the reactor plugged within < 5 min (at a total flow rate of 0.5 ml/min). Even ultra-sonication (placing the mixers and tubing in an ultra-sonicated bath) increased the operation time only marginally.

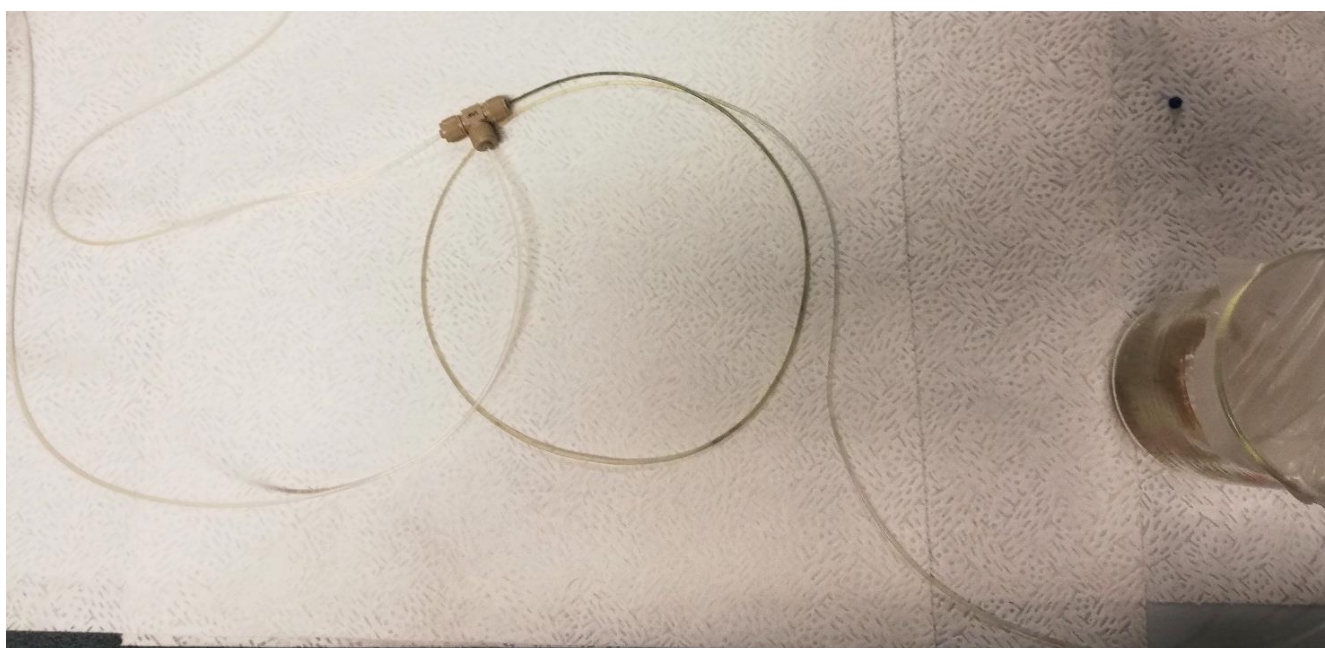


**Figure S12:** Image of room temperature mixing of precursor (1) and base (2) solutions via a P-890 micro mixer. The mixer plugged soon after initiating the reaction and the PTFE tubing connected to the mixer outlet showed severe fouling (see black and greenish depositions at the mixer outlet tubing); Solutions flowing from left to right.

## S15 Flow synthesis reproducibility

The flow synthesis was repeated to study the robustness of the reactor and synthesis. The entire synthetic procedure was repeated (from solution preparation to sample analysis). TEM analysis (see **Figure S13a**), revealed again a clear effect of TEPA only for the highest TEPA : Fe ratio (1 : 15.6). The particle iron concentration was comparable for all IONP solutions synthesised at 0.2 ml/min precursor solution with 1.12, 1.09 and 1.05 mg<sub>Fe-IONP</sub>/ml<sub>sol</sub> for 0, 0.02 and 0.04 ml/min of the TEPA solution, and 0.50 mg<sub>Fe-IONP</sub>/ml<sub>sol</sub> (at 0.04 ml/min TEPA solution) after halving the precursor solution feed rate, corresponding to TEPA : Fe ratios of 0, 1:62.5, 31.3, and 15.6 respectively. These correspond to a precursor conversion (assuming no other product than IONPs) of 81%, 80%, 79% and 66% showing a slight decrease with increasing TEPA levels. All IONPs solutions synthesised showed excellent colloidal stability after ultra-sonication with hydrodynamic diameters of  $D_h = 125, 147, 143, \text{ and } 173 \text{ nm}$  for syntheses at TEPA : Fe ratios of 0, 1:62.5, 31.3, and 15.6 respectively. The IONPs synthesised in this repeated flow synthesis yielded ILP values of 3.2, 3.4, 3.1 and 2.0 nH m<sup>2</sup> kg<sub>Fe</sub><sup>-1</sup> (see **Figure S13b**). All particle iron concentrations, conversions, hydrodynamic diameters and heating rates were very similar to those obtained in the first synthesis at the same TEPA : Fe ratios (see **Figure 3**).

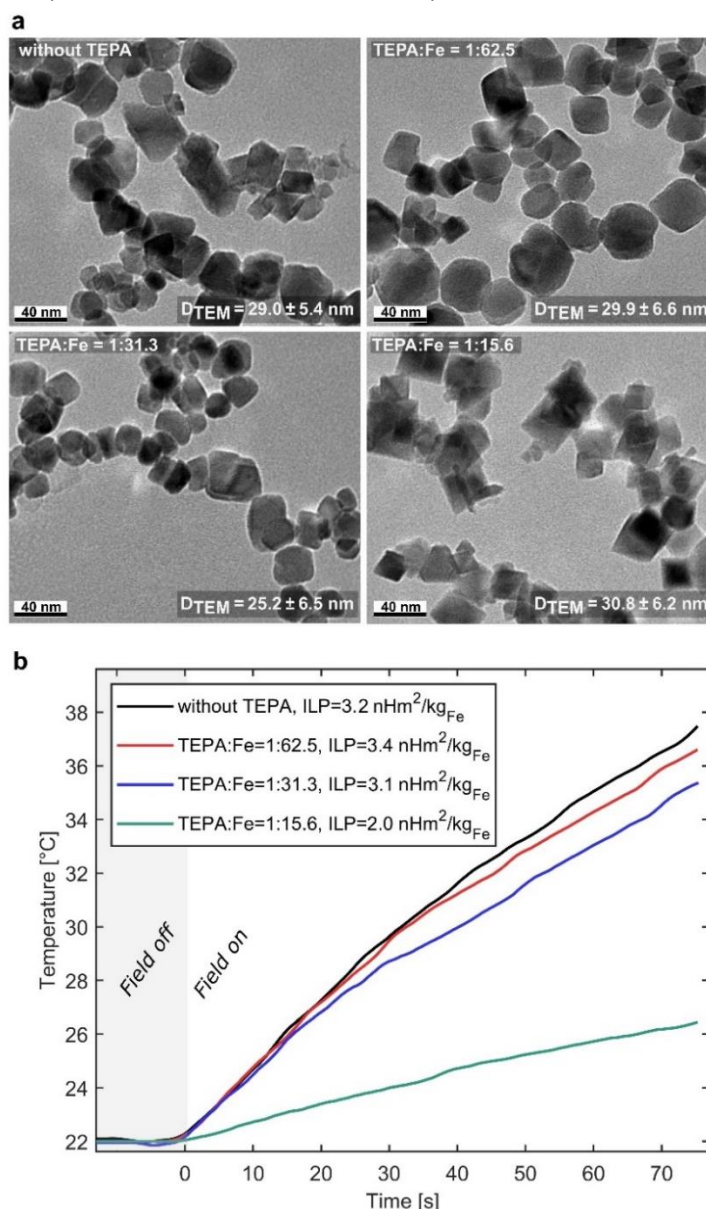


**Figure S13:** IONP solutions synthesised using the three-phase reactor platform operated identically as for the results shown in Figure 3. **(a)** TEM analysis of IONPs synthesised at the different TEPA : Fe ratios. **(b)** Corresponding heating profiles (of washed IONP solutions) with ILP values in the legend.